Electronic Supplementary Information

Synthesis, photophysical and cytotoxicity evaluations of DNA targeting agents based on 3-amino-1,8-naphthalimide derived Tröger's bases

Samantha Murphy,[a] Sandra A. Bright,[b] Fergus E. Poynton,[a] Thomas McCabe,[a] Jonathan A. Kitchen,[a] Emma B. Veale,*[a] D. Clive Williams*[b] and Thorfinnur Gunnlaugsson*[a]

Figure S1. Crystal Structures of 6-10.

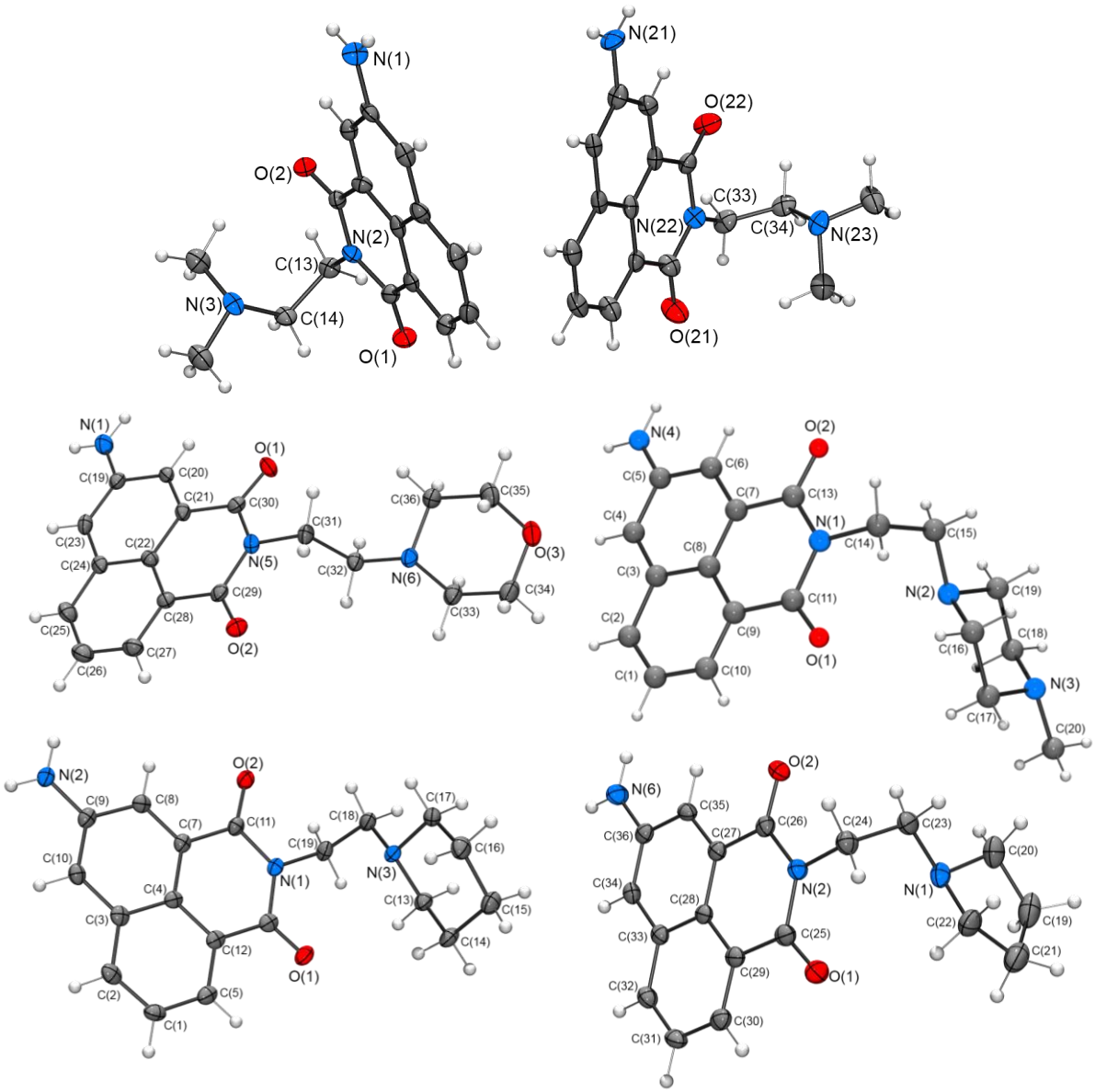

Figure S2. Hydrogen bonding of 9.

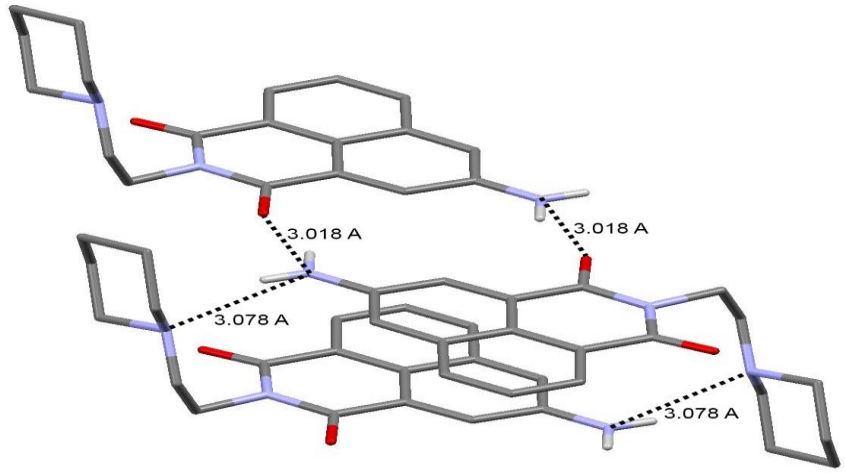

Figure S3. Hydrogen bonding of 8.

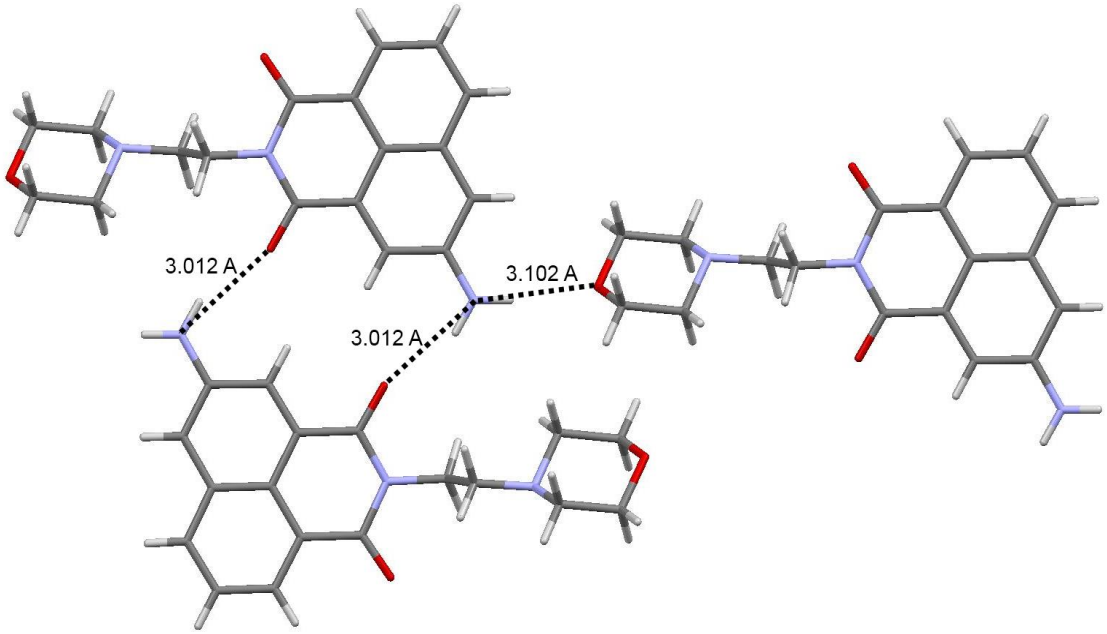

Table S1. Crystal data and structure refinement for 6

Empirical formula	$C_{18}\ H_{19}\ N_3\ O_2$
Formula weight	309.36
Temperature	118(2) K
Wavelength	0.71075 Å
Crystal system	Monoclinic
Space group	P2(1)/c

Unit cell dimensions	a = 6.6599(17) Å	α= 90°.
	b = 21.310(5) Å	β= 99.174(4)°.
	c = 11.054(3) Å	γ = 90°.
Volume	1548.7(7) $Å^3$	
Z	4	
Density (calculated)	1.327 Mg/m^3	
Absorption coefficient	0.088 mm^{-1}	
F(000)	656	
Crystal size	0.32 x 0.21 x 0.14 mm^3	
Theta range for data collection	1.91 to 25.00°.	
Index ranges	-7<=h<=7, -24<=k<=25, -12<=l<=13	
Reflections collected	12422	
Independent reflections	2692 [R(int) = 0.0456]	
Completeness to theta = 25.00°	98.8 %	
Absorption correction	Semi-empirical from equivalents	
Max. and min. transmission	1.0000 and 0.7695	
Refinement method	Full-matrix least-squares on F^2	
Data / restraints / parameters	2692 / 0 / 208	
Goodness-of-fit on F^2	1.169	
Final R indices [I>2sigma(I)]	R1 = 0.0583, wR2 = 0.1641	
R indices (all data)	R1 = 0.0845, wR2 = 0.1973	
Largest diff. peak and hole	0.438 and -0.460 e.$Å^{-3}$	

Table S2. Crystal data and structure refinement for 8.

Empirical formula	C_{18} H_{19} N_3 O_3	
Formula weight	325.36	
Temperature	108(2) K	
Wavelength	0.71075 Å	
Crystal system	Monoclinic	
Space group	P2(1)/c	
Unit cell dimensions	a = 5.5440(18) Å	α= 90°.
	b = 23.166(8) Å	β= 102.769(4)°.
	c = 12.365(4) Å	γ = 90°.
Volume	1548.8(9) $Å^3$	
Z	4	
Density (calculated)	1.395 Mg/m^3	
Absorption coefficient	0.097 mm^{-1}	
F(000)	688	

Crystal size	0.39 x 0.31 x 0.24 mm^3
Theta range for data collection	2.44 to 25.00°.
Index ranges	-6<=h<=6, -27<=k<=27, -14<=l<=14
Reflections collected	7067
Independent reflections	2638 [R(int) = 0.0437]
Completeness to theta = 25.00°	96.5 %
Absorption correction	Semi-empirical from equivalents
Max. and min. transmission	1.0000 and 0.7933
Refinement method	Full-matrix least-squares on F^2
Data / restraints / parameters	2638 / 0 / 217
Goodness-of-fit on F^2	1.123
Final R indices [I>2sigma(I)]	R1 = 0.0599, wR2 = 0.1700
R indices (all data)	R1 = 0.0907, wR2 = 0.2225
Largest diff. peak and hole	0.423 and -0.373 e.$Å^{-3}$

Table S3. Crystal data and structure refinement for 9

Empirical formula	C_{19} H_{21} N_3 O_2	
Formula weight	323.39	
Temperature	108(2) K	
Wavelength	0.71075 Å	
Crystal system	Monoclinic	
Space group	P2(1)/c	
Unit cell dimensions	a = 6.962(2) Å	α= 90°.
	b = 14.046(5) Å	β= 95.843(4)°.
	c = 16.346(6) Å	γ = 90°.
Volume	1590.1(9) $Å^3$	
Z	4	
Density (calculated)	1.351 Mg/m^3	
Absorption coefficient	0.089 mm^{-1}	
F(000)	688	
Crystal size	0.39 x 0.25 x 0.18 mm^3	
Theta range for data collection	2.51 to 24.99°.	
Index ranges	-7<=h<=8, -16<=k<=15, -19<=l<=19	
Reflections collected	12869	
Independent reflections	2792 [R(int) = 0.0406]	
Completeness to theta = 24.99°	99.6 %	
Absorption correction	Semi-empirical from equivalents	
Max. and min. transmission	1.0000 and 0.7695	

Refinement method	Full-matrix least-squares on F^2
Data / restraints / parameters	2792 / 0 / 217
Goodness-of-fit on F^2	1.202
Final R indices [I>2sigma(I)]	R1 = 0.0588, wR2 = 0.1139
R indices (all data)	R1 = 0.0697, wR2 = 0.1190
Largest diff. peak and hole	0.287 and -0.354 e.Å^{-3}

Figure S4. ^{1}H NMR spectrum ($CDCl_3$, 600 MHz) of 1

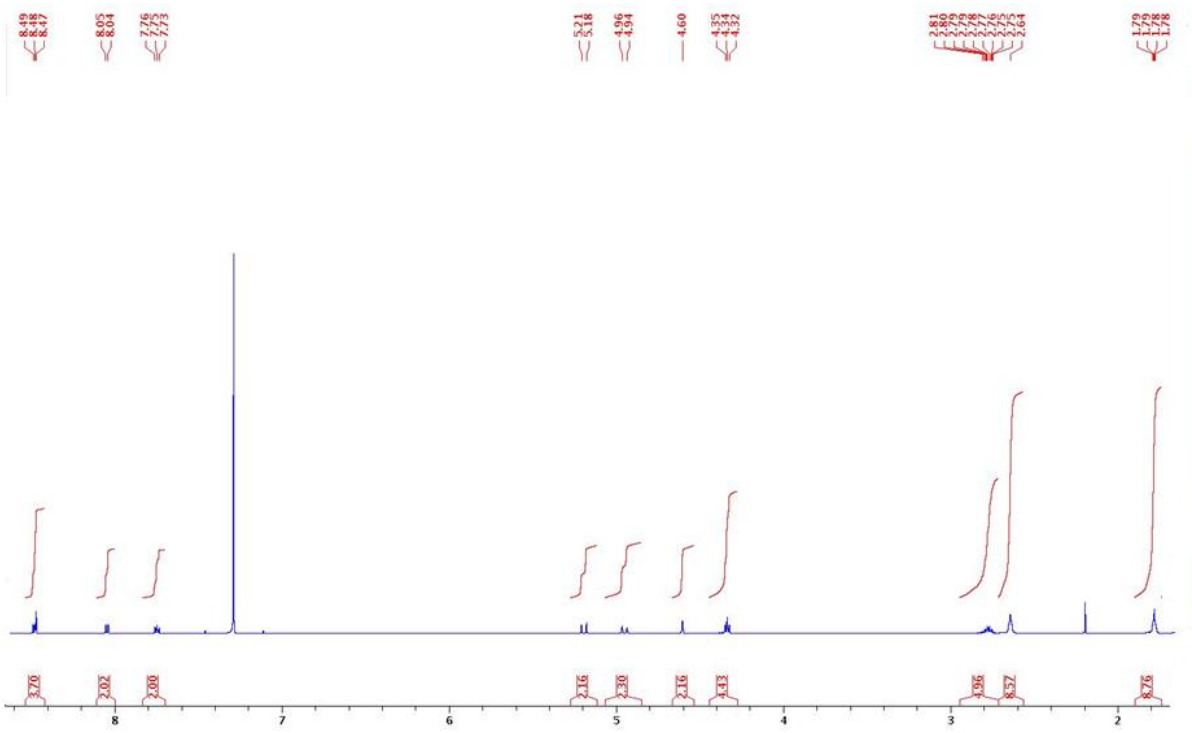

Figure S5. ^{1}H NMR spectrum ($CDCl_3$, 400 MHz) of 3

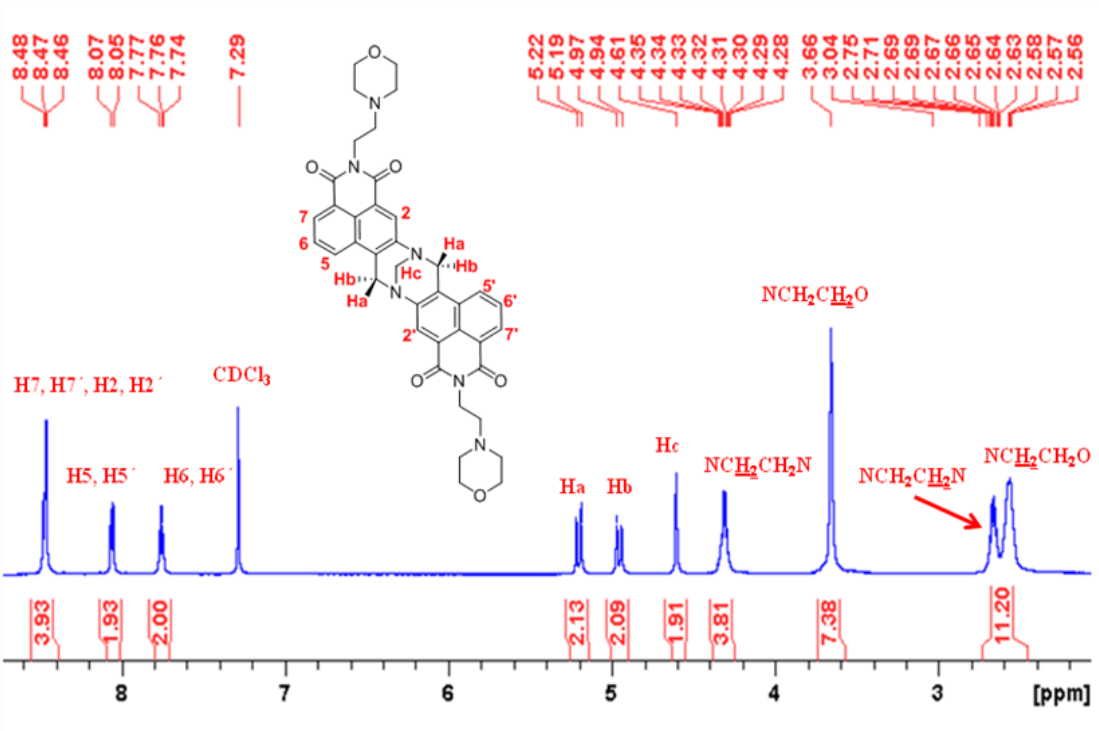

Figure S6. ^{1}H NMR spectrum ($CDCl_3$, 400 MHz) of 2

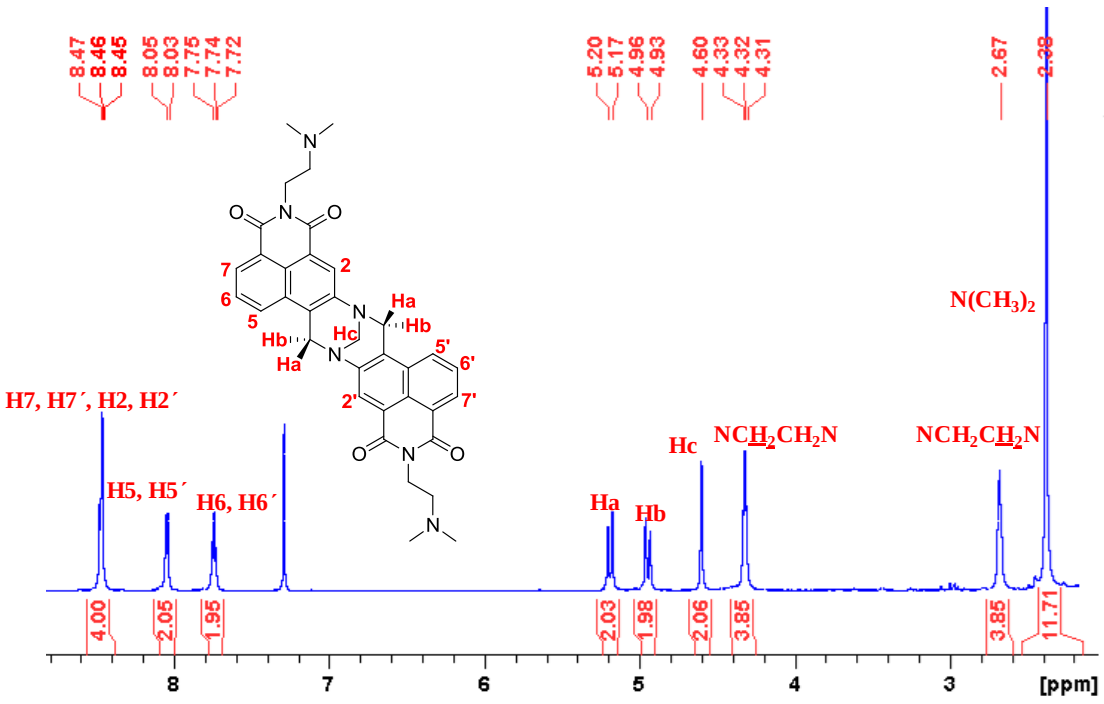

Figure S7. ^{1}H NMR spectrum ($CDCl_3$, 400 MHz) of 4

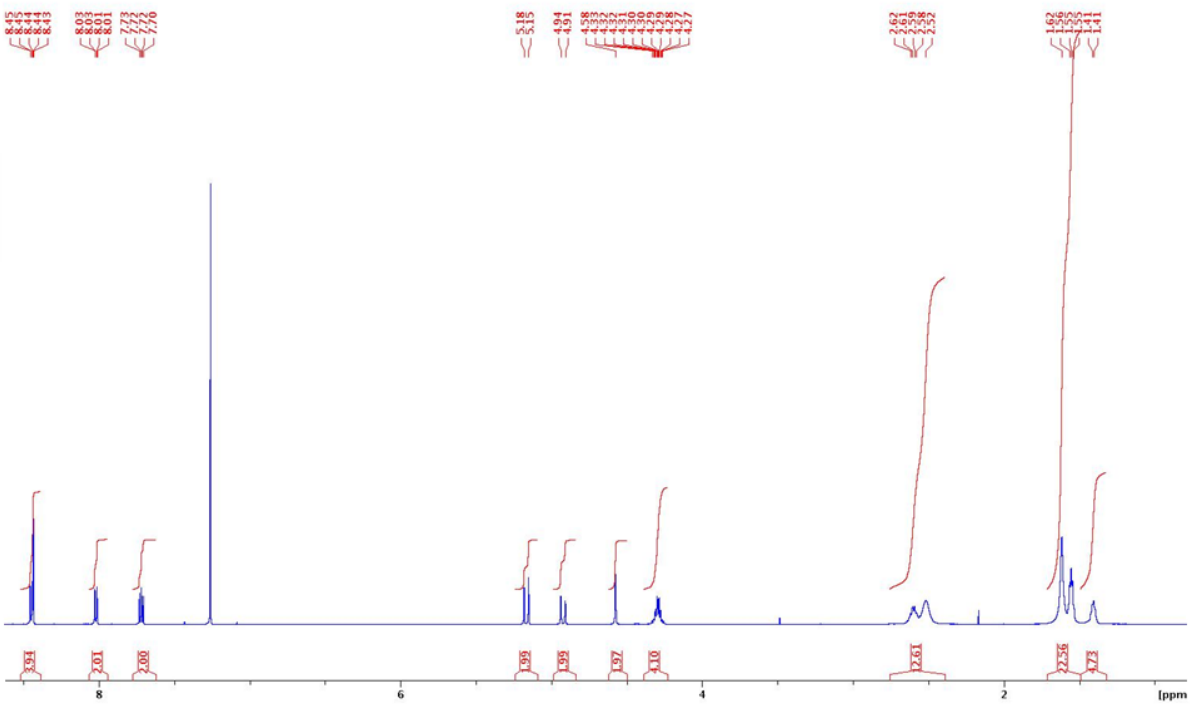

Figure S8. ^{1}H NMR spectrum ($CDCl_3$, 400 MHz) of 5

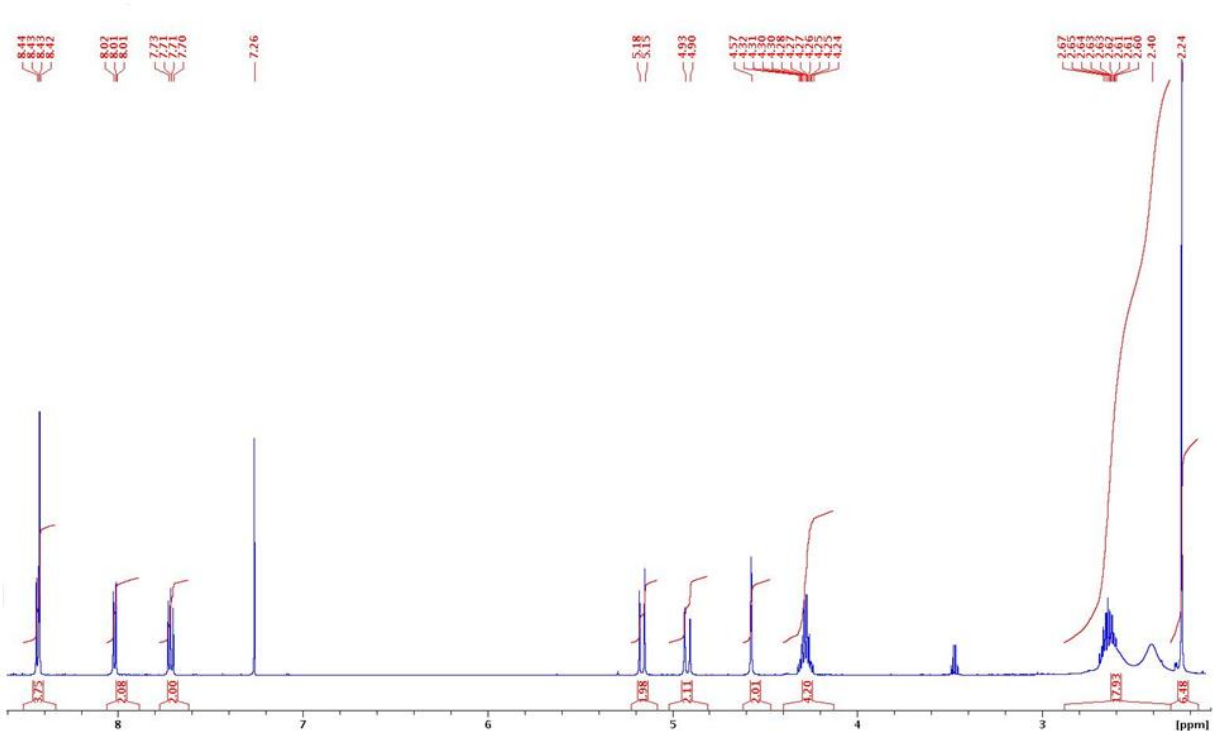

Figure S9. Absorption spectra of 2 in solvents of varying polarity.

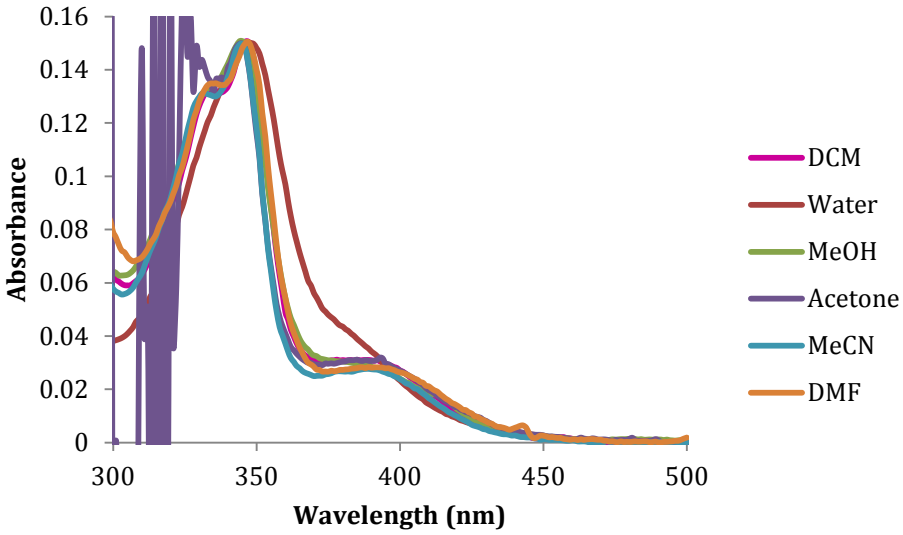

Figure S10. Emission spectra of 2 in solvents of varying polarity (excitation at 347 nm)

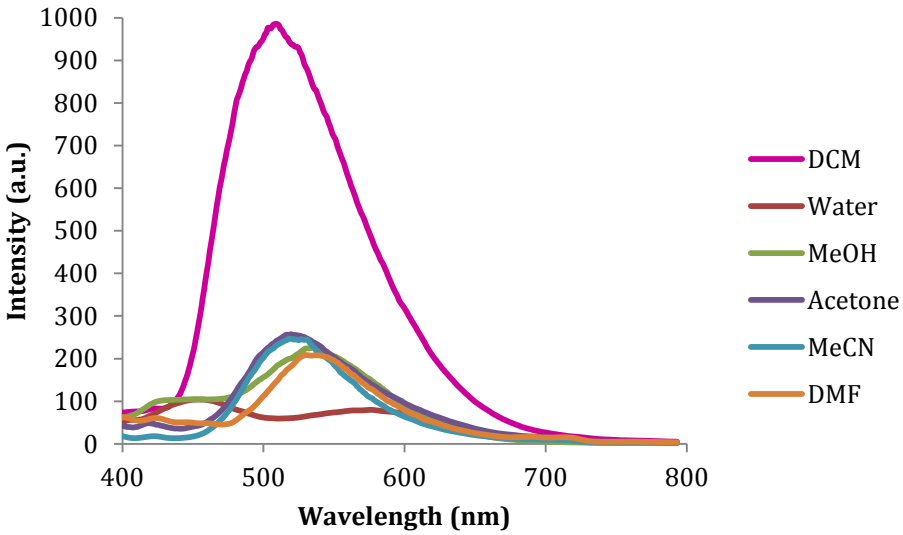

Figure S11. Absorption spectra of 3 in solvents of varying polarity.

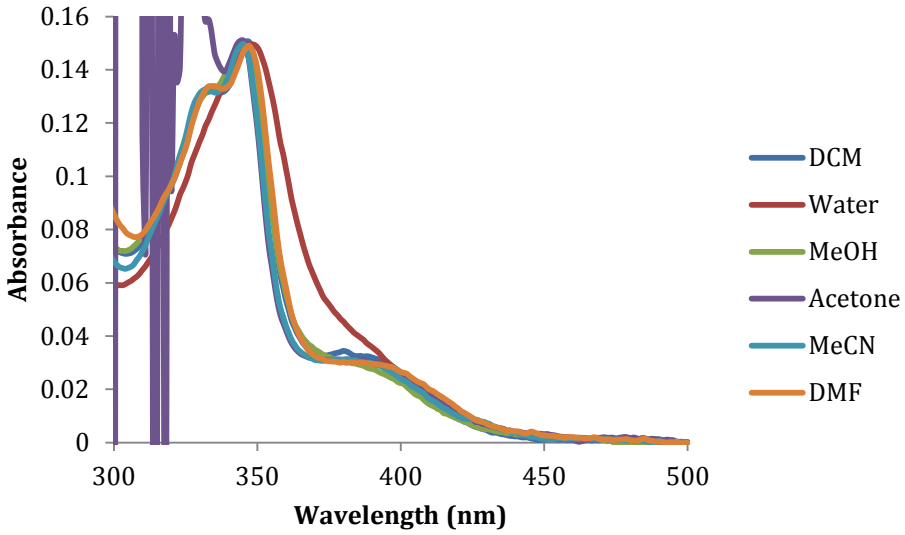

Figure S12. Emission spectra of 3 in solvents of varying polarity (excitation at 347 nm)

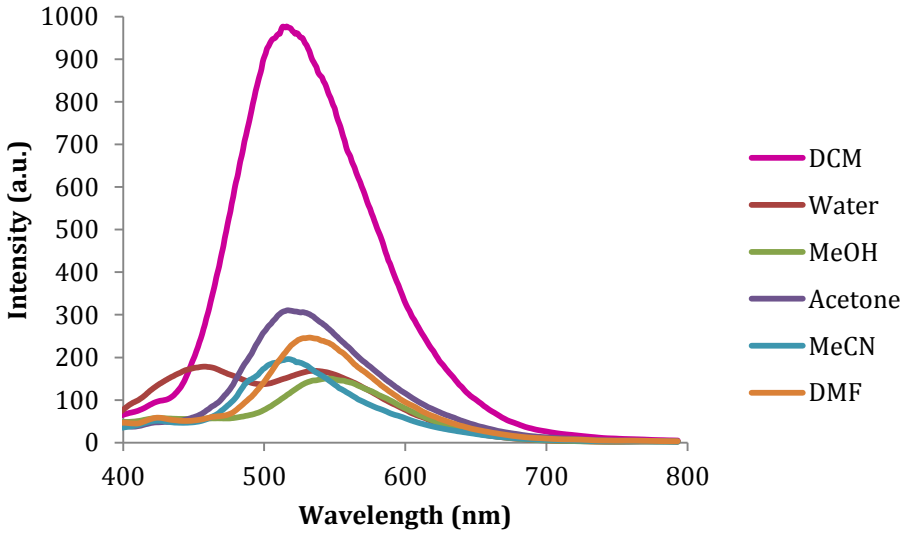

Figure S13. Absorption spectra of 5 in solvents of varying polarity.

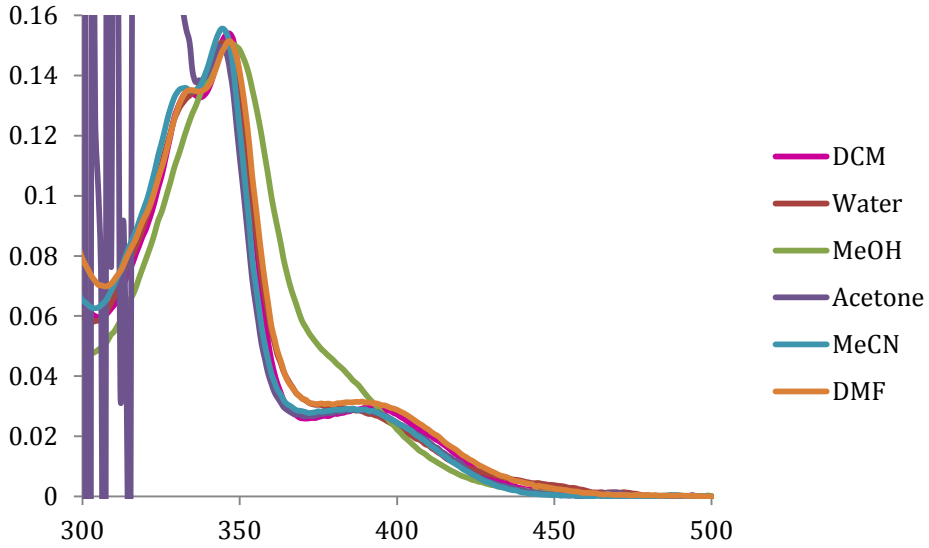

Figure S14. Emission spectra of 5 in solvents of varying polarity (excitation at 347 nm).

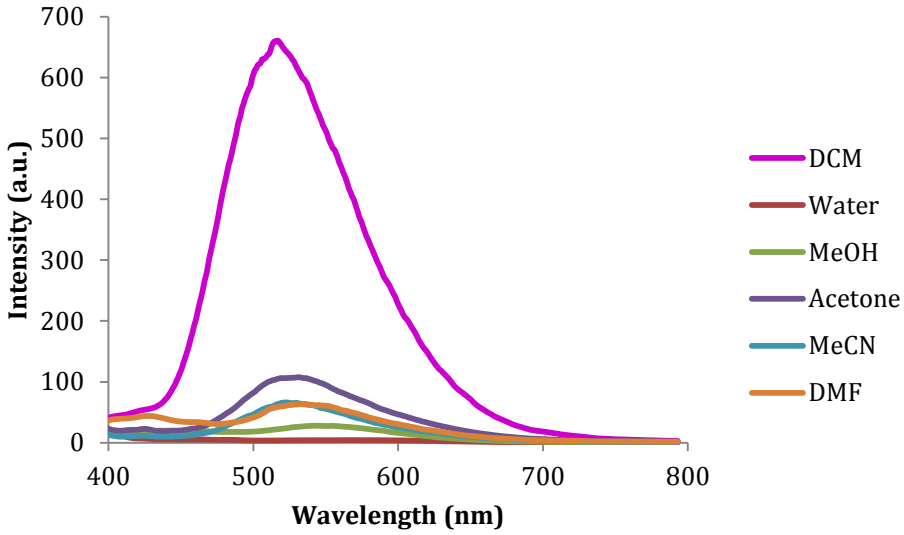

Figure S15. Absorption spectra of 4 in solvents of varying polarity.

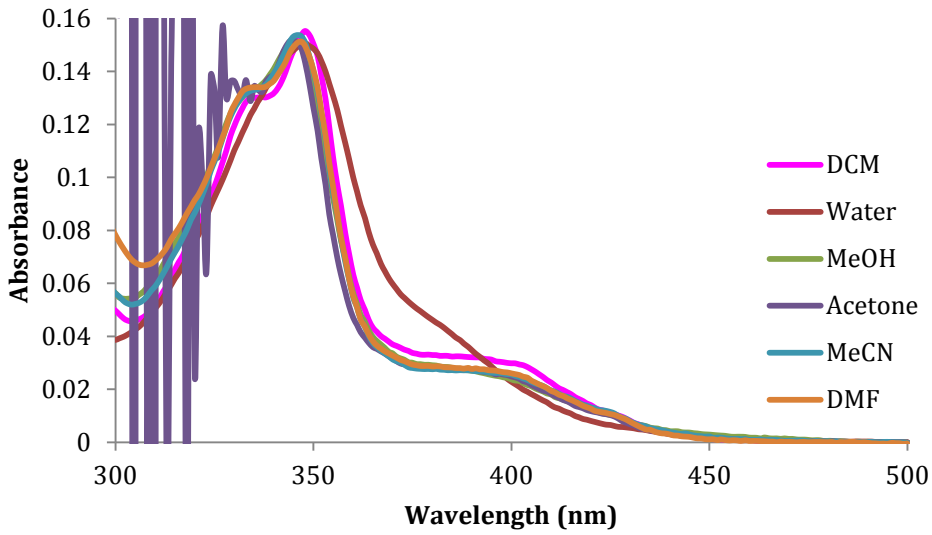

Figure S16. Emission spectra of 4 in solvents of varying polarity (excitation at 347 nm).

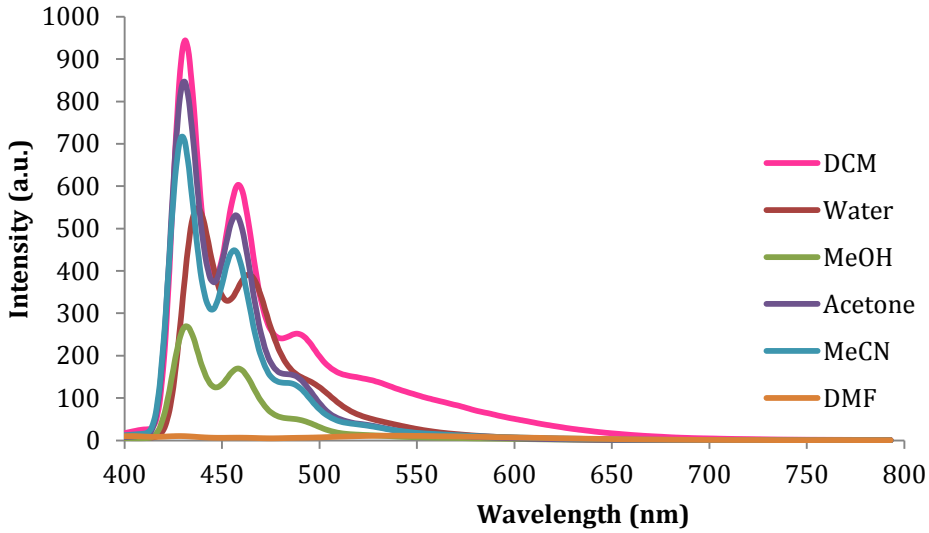

Figure S17. Emission spectra of 6 in solvents of varying polarity (excitation at 390 nm) in CH_2Cl_2 (-), CH_3OH (-), H_2O (-), CH_3CN (-), Acetone (-) and DMF (-) where λ_{maxFLU} = 481, 555, 591, 505, 503 and 530 nm, respectively.

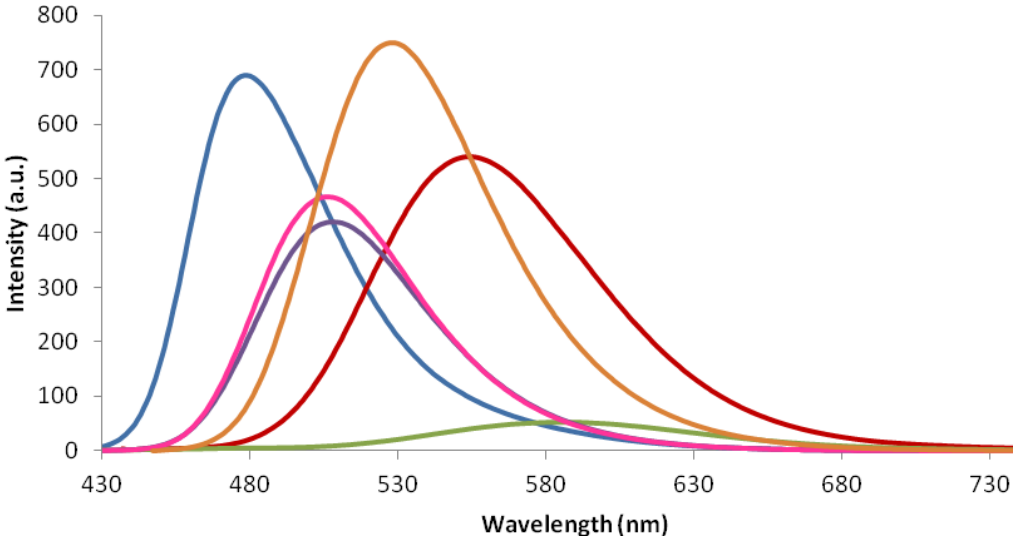

Figure S18. Absorption spectra of 7 as a function of pH

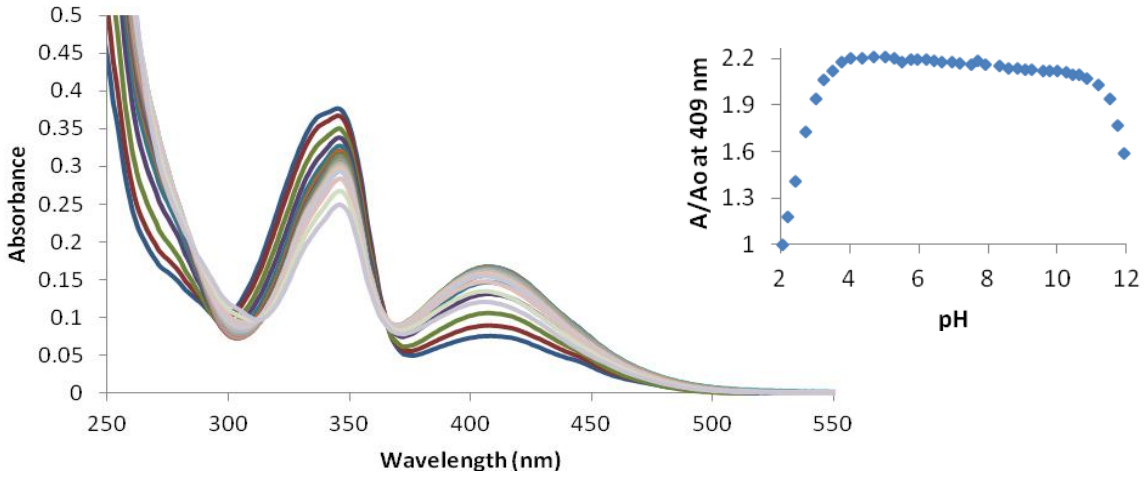

Figure S19. The absorption spectra of 2 (5.3 µM) in (a) 10 mM phosphate buffer and 50 mM NaCl and (b) 10 mM phosphate buffer and 160 mM NaCl upon titration with ct-DNA (0- 272 µM)

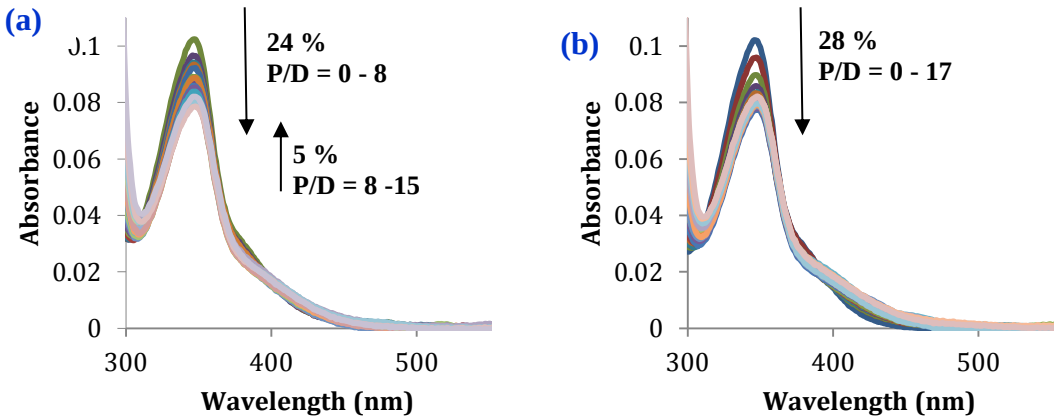

Figure S20. Plot of the changes in the absorbance of 2 in 10 mM phosphate buffer (♦) and along with 50 mM NaCL (♦) and along with 160 mM NaCl (♦) versus P/D @ 347 nm.

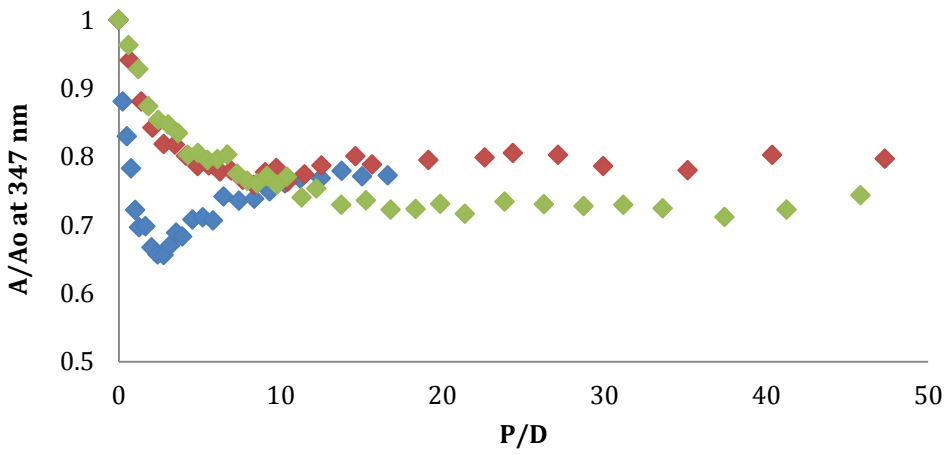

Figure S21. Plot of the changes in the absorbance of 5 in 10mM phosphate buffer as a function of P/D in the absence of NaCl (♦), the presence of 50 mM NaCl (♦) and the presence of 160 mM NaCl (♦).

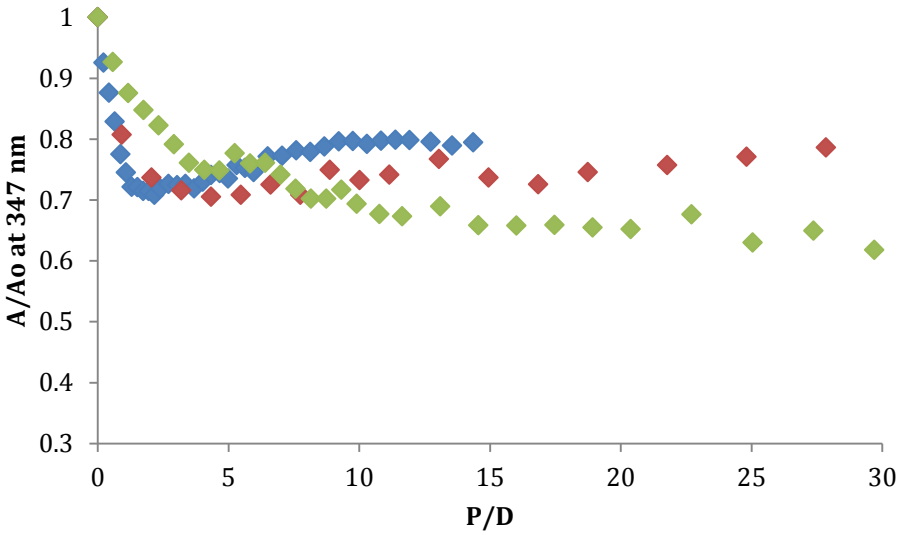

Figure S22. Plot of the changes in the absorbance of 4 in 10 mM phosphate buffer as a function of P/D in the absence of NaCl (♦), the presence of 50 mM NaCl (♦) and the presence of 160 mM NaCl (♦).

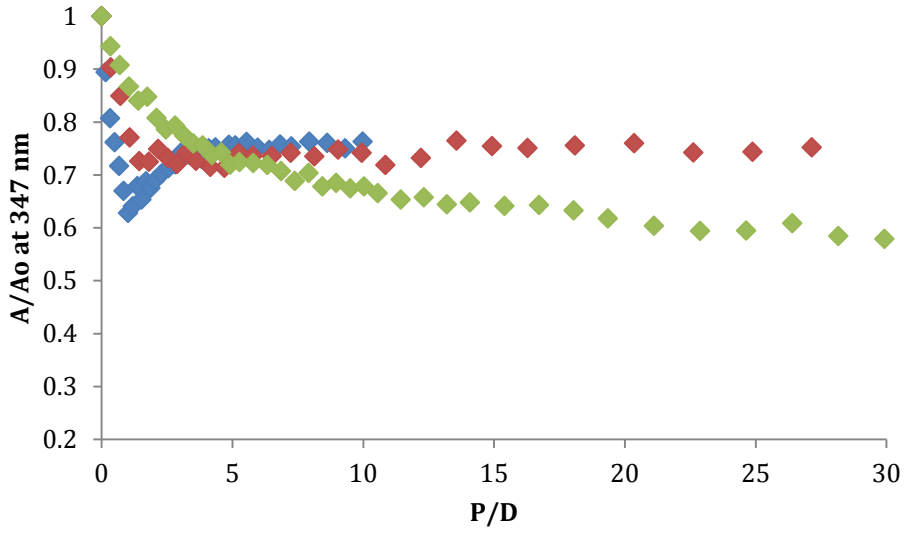

Figure S23. Plot of the changes in the absorbance of 1 in 10 mM phosphate buffer as a function of P/D in the absence of NaCl (♦), the presence of 50 mM NaCl (♦) and the presence of 160 mM NaCl (♦).

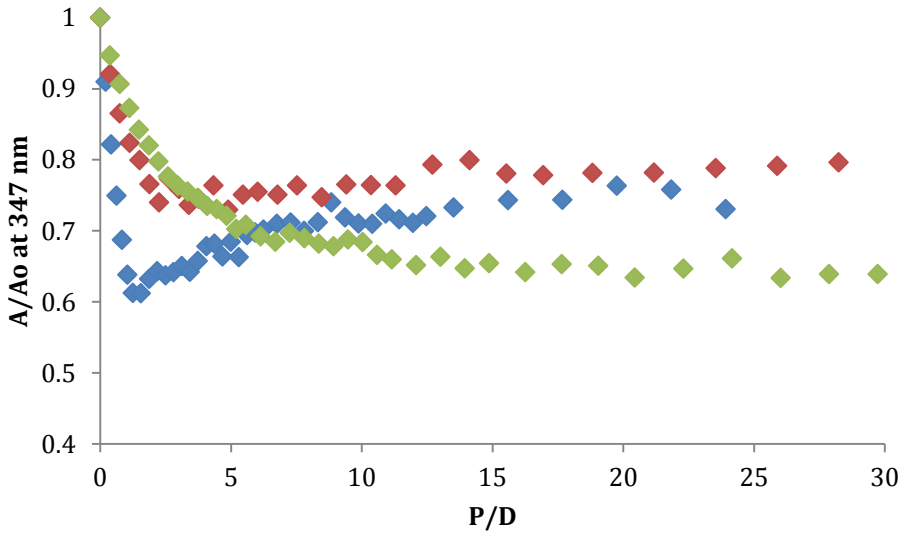

Table S4. Binding constants determined for 2 bound to ct-DNA in 10 mM phosphate buffer and competitive media using the Bard Model.[22]

NaCl (mM)	Kb (10^6 M^{-1})	n (bp)	R^2
0	8.51 (± 5.34)	0.22 (±0.01)	0.99
50	2.24 (± 1.09)	0.21 (± 0.02)	0.98
160	0.41 (±0.12)	0.63 (± 0.10)	0.98

Figure S24. Plot of $(\varepsilon_a-\varepsilon_f)/(\varepsilon_b-\varepsilon_f)$ versus ct-[DNA] for 2 (a), 5 (b), 4 (c) and 1 (d) and the corresponding non-linear fits to Bard model

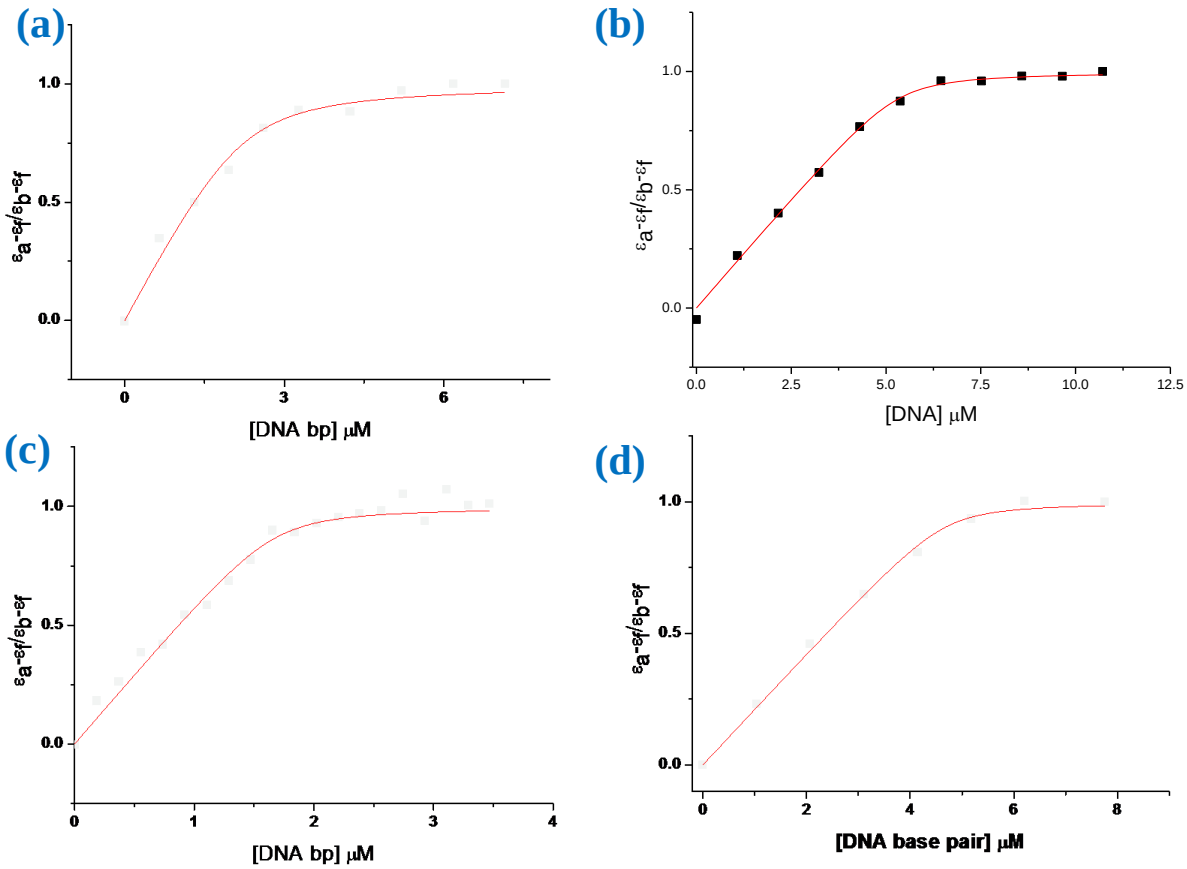

Figure S25. The absorption spectrum of 7 (9.3 μM) in 10 mM phosphate buffer (pH 7.4) with increasing concentration of ct-DNA (0 – 228.2 μM).

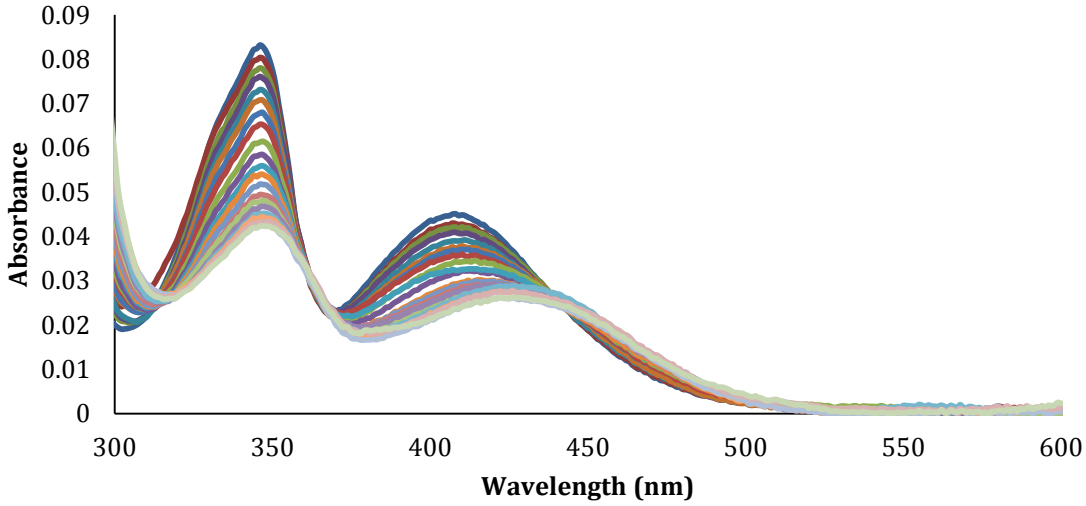

Figure S26. Fluorescence emission spectrum (λ_{Ex} = 408 nm) of 7 (9.3 µM) in 10 mM phosphate buffer (pH 7.4) upon successive addition of ct-DNA (0 – 228.2 µM). Inset: Plot of changes in emission spectrum of 7 as a function of P/D at 582 nm.

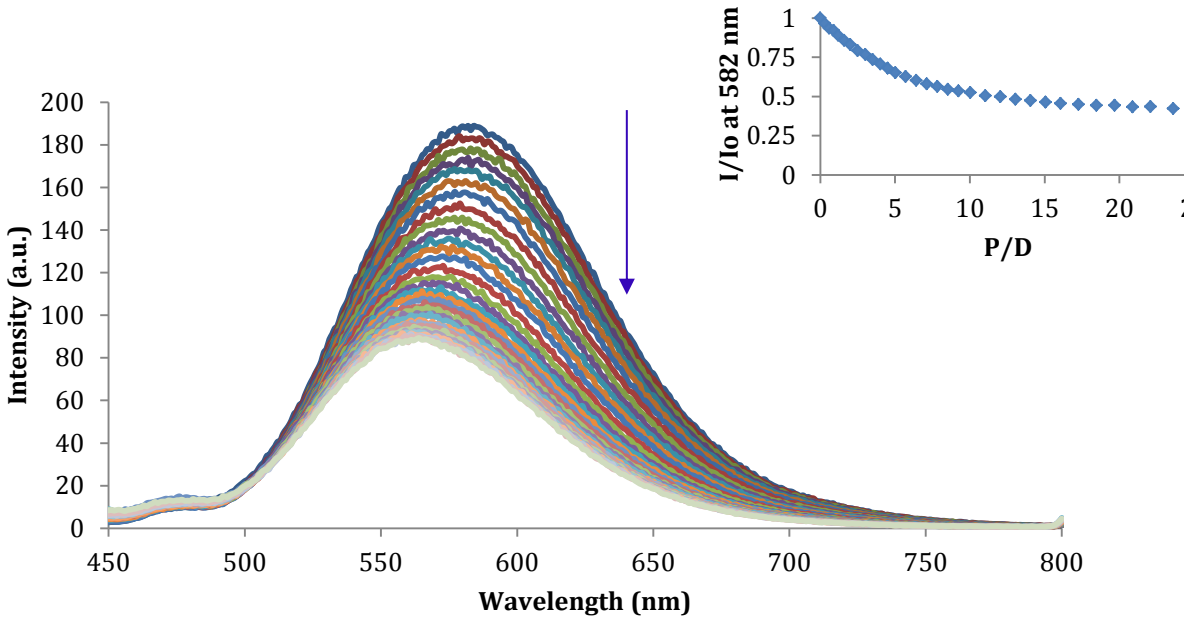

Table S5. Summary of emission properties observed for 6-10 upon the addition of ct-DNA in 10 mM phosphate buffer (pH 7.4). [a] λ_{maxF} is the wavelength of maximum intensity for the free compound. [c] λ_{maxB} is the wavelength of maximum intensity for the bound compound.

Property	7	8	10	9	6
λ_{maxF} (nm) [a]	582	587	581	583	585
λ_{maxB} (nm) [b]	558	574	552	564	559
Hypochromism (%)	70	64	35	51	56
Hypsochromic Shift	24	13	29	19	26

Table S6. Binding constants K_b and binding site sizes n obtained from emission spectra determined using the McGhee and von Hippel binding model.

Compound	K_b ($\times 10^6$ M^{-1})	n(bp)	R^2
2	0.22 (± 0.01)	1.15 (± 0.04)	0.88
5	5.64 (± 0.24)	0.42 (± 0.01)	0.76
4	0.78 (± 0.02)	1.19 (± 0.03)	0.95

Table S7. Binding constants K_b and binding site sizes n obtained from emission spectra at different ionic strength determined using the McGhee and von Hippel Binding Model.

Compound	50 mM NaCl		160mM NaCl	
	K_b (10^6 M^{-1})	**n** (bp)	**K_b** (10^6 M^{-1})	**n** (bp)
2	0.15 (± 0.01)	2.50 (± 0.21)	0.12 (± 0.01)	1.23 (± 0.12)
5			0.034 (±0.007)	0.70 (±0.03)
4	0.67 (± 0.03)	1.79 (±0.05)	0.21 (± 0.004)	1.73 (± 0.04)

Table S8. Binding constants K_b and binding site sizes n obtained from absorption spectra determined, where possible, for 6-10 bound to ct-DNA in 10 mM phosphate buffer at pH 7.4, using the Bard and Mc Ghee and von Hippel models. [a] An accurate K_b could not be determined.

Compound	Bard		McGhee and von Hippel	
	K_b ($\times 10^6$ M^{-1})	n(bp)	K_b ($\times 10^6$ M^{-1})	n(bp)
7	1.22 (± 0.30)	1.24 (±0.07)	0.37 (± 0.02)	1.82 (±0.06)
8	0.11 (± 0.05)	1.27 (± 0.09)	0.06 (±0.003)	2.69 (±0.08)
10	0.25 (±0.07)	0.90 (± 0.13)	0.14 (± 0.01)	2.21 (±0.01)
9	0.57 (±0.11)	0.78 (± 0. 05)	0.35 (± 0.01)	1.58 (±0.03)
6	_____ [a]	_____ [a]	0.30 (± 0.03)	2.46 (± 0.08)

Table S9. Binding constants K_b and binding site sizes n obtained from emission spectra determined for 6-10, where possible, using the McGhee-von Hippel binding model. [a] Using the data obtained no accurate binding constant could be determined.

Compound	K_b ($\times 10^5$ M^{-1})	n(bp)	R^2
7	0.22 (± 0.01)	2.41 (± 0.01)	0.98
8	_____ [a]	_____ [a]	0.88
10	0.14 (± 0.01)	2.21 (± 0.10)	0.89
9	0.25 (± 0.01)	1.75 (± 0.05)	0.94
6	0.86 (± 0.03)	0.65 (± 0.01)	0.92

Figure S27. Thermal denaturation curves and T_m values of ct-DNA (150 µM) in 10 mM phosphate buffer at pH 7.4 in the absence (-) and presence of 2 (-), 5 (-), 4 (-) and 1 (-), all at a P/D ratio of 10.

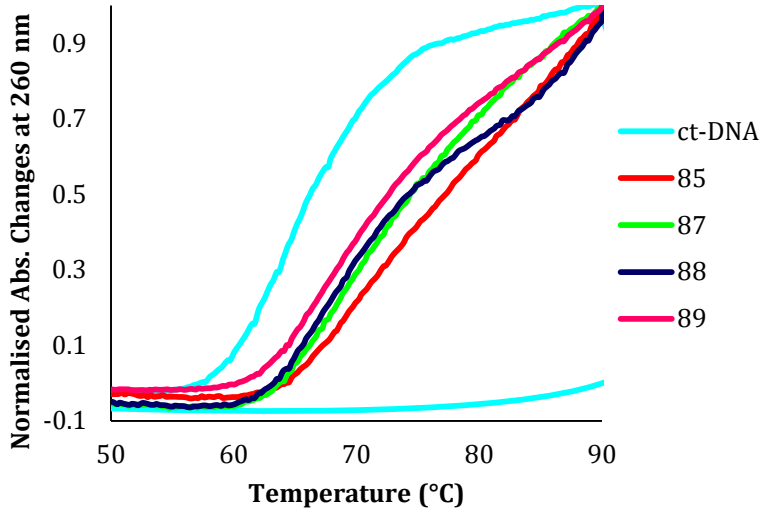

Compound	T_m (°C)
***ct*-DNA**	68
1	>75
2	>75
4	>75
5	>75

Figure S28. CD spectra of ct-DNA (150 µM) (-) in the presence of 2 at P/D ratios of 2.5 (-), 5 (-), 10(-) and 20 (-).

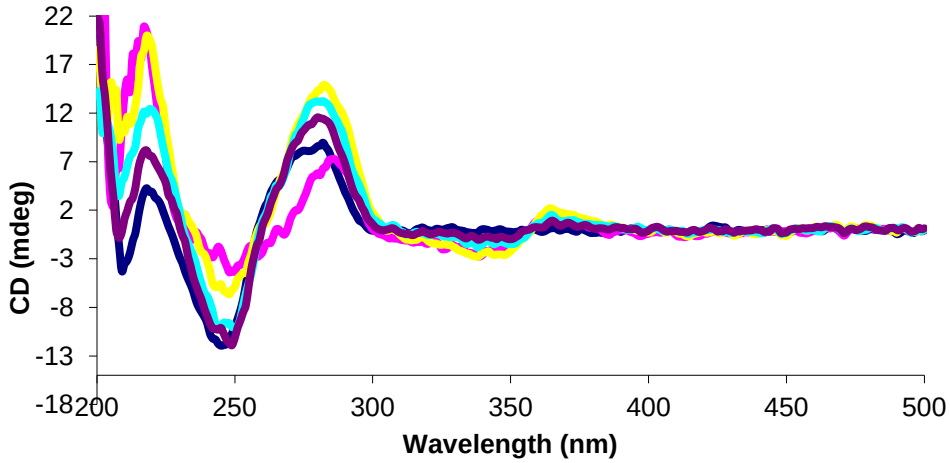

Figure S29. CD spectra of ct-DNA (150 µM) (-) in the presence of 4 at P/D ratios of 2.5 (-), 5 (-), 10(-) and 20 (-) in phosphate buffer (pH 7.4)

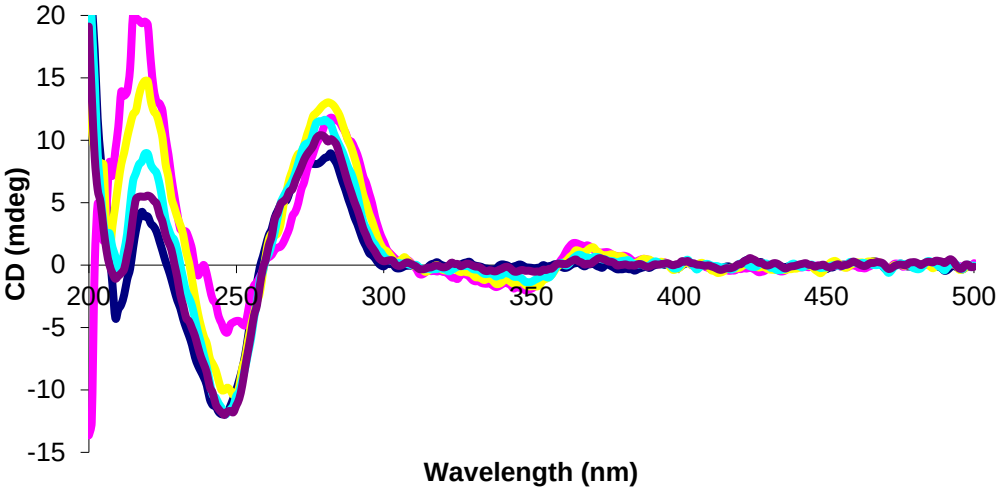

Figure S30. CD spectra of ct-DNA (150 µM) (-) in the presence of 5 at P/D ratios of 2.5 (-), 5 (-), 10(-) and 20 (-).

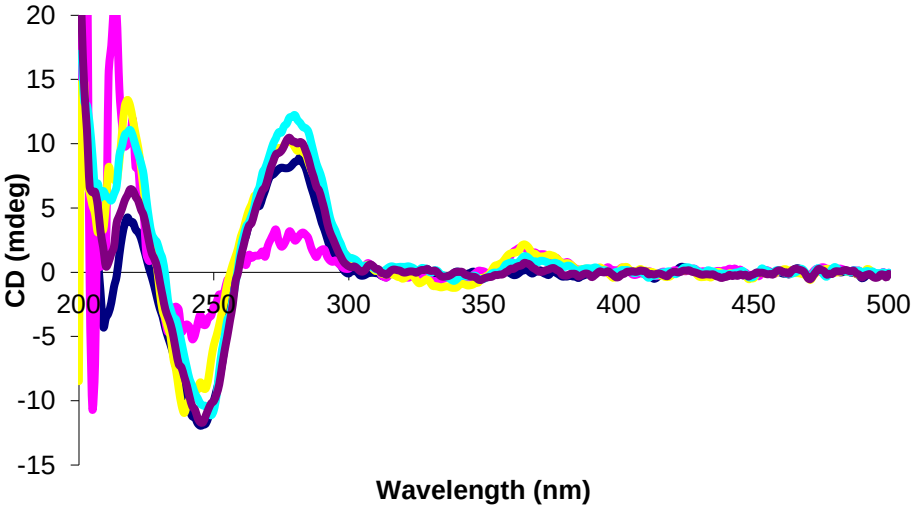

Figure S31. LD spectra of ct-DNA (400 µM) in 10 mM phosphate buffer in the absence (-) and presence of 1 at P/D ratios of 2.5 (-), 5 (-), 10 (-) and 20 (-).

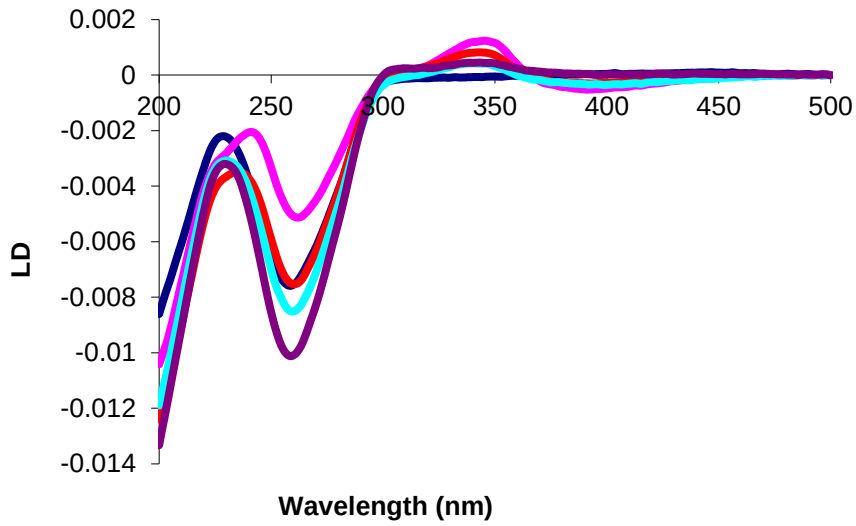

Figure S32. LD spectra of ct-DNA (400 µM) (◆) in the presence of 2 at P/D ratios of 2.5 (◆), 5 (◆), 10(◆) and 20 (◆) in phosphate buffer (pH 7.4).

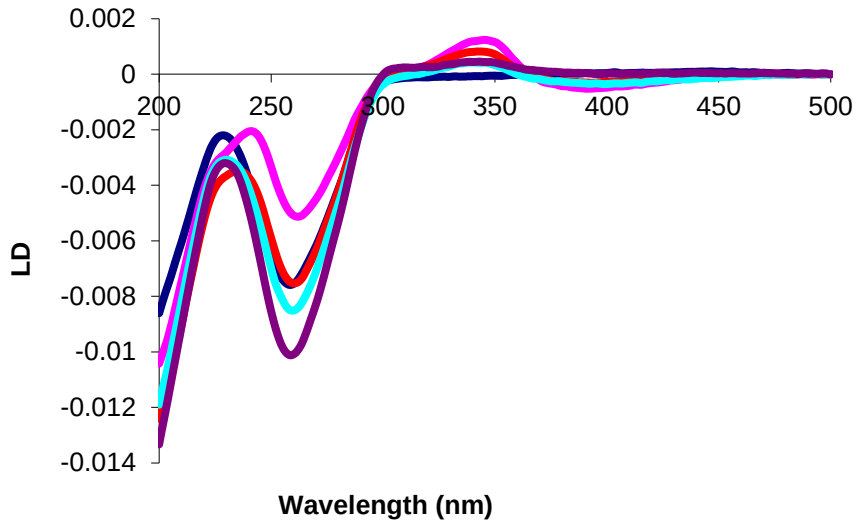

Figure S33. LD spectrum of 6 at a P/D ratio of 2.5 in 10 mM phosphate buffer at pH 7.4, [ct-DNA]=400 µM.